Received: 15 July 2024 | Revised: 15 August 2024 | Accepted: 25 August 2024

DOI: 10.1002/app.56241

RESEARCH ARTICLE

Journal of Applied Polymer Science WILEY

On the suitability of the α-relaxation as novel trigger for a shape memory polymer

Michail Maricanov | Roman Becker | Robert David Ludwig Jerusalem | Joerg Christian Tiller | Frank Katzenberg

Biomaterials and Polymer Science, Department of Biochemical and Chemical Engineering, Technical University Dortmund, Dortmund, Germany

Correspondence
Frank Katzenberg, Biomaterials and Polymer Science, Department of Biochemical and Chemical Engineering, Technical University Dortmund, 44221 Dortmund, Germany.
Email: frank.katzenberg@tu-dortmund.de

Funding information
Deutsche Forschungsgemeinschaft, Grant/Award Number: DFG KA1813/5-1

Abstract

Shape memory polymers typically utilize the glass transition or melting temperature to switch from one shape to another. The goal of this work is to check if the α-relaxation, which is attributed to the migration of chains through lamellar crystals, can be utilized as novel switch for any crosslinkable semi-crystalline thermoplastic. Using cross-linked low-density polyethylene (x-LDPE) as an example, it is shown that the α-relaxation is indeed suitable as switch, when the polymer is crystallized under strain to an intermediate shape. It is demonstrated that post-stretching at a temperature between the α-relaxation and the melting temperature, followed by subsequent cooling to room-temperature switches x-LDPE from the intermediate to a temporary shape and that reheating to this temperature initiates the retraction back to the intermediate shape. Switching between intermediate and temporary shapes is shown to be accompanied by a reversible change in morphology.

KEYWORDS

applications, crosslinking, glass transition, structure-property relationships, thermal properties

1 | INTRODUCTION

A material that can respond and adapt to its environment is referred to as a smart, responsive, or adaptable material. Shape memory polymers, which can be programmed into a stable temporary shape and usually return completely to their original shape after being triggered, belong to the group of such smart materials and have been intensively researched for several decades.[1–7] The ability of a thermally triggered shape memory polymer (SMP) to stabilize a highly deformed temporary shape and fully recover its original shape when heated above its trigger temperature usually requires two prerequisites: (1) The polymer can be reversibly entropy-elastically deformed. (2) The entropy-driven retraction forces of the oriented amorphous phase can be compensated when the SMP is programmed to its temporary form. Point 1 can usually be ensured by sufficient chemical crosslinking. Point 2 can be satisfied either upon freezing of the amorphous phase below the classic glass transition temperature T_g (glass-forming SMP) or upon forming crystals in sufficient amount below the melting temperature T_m (crystalline-based SMP). Unsurprisingly, the trigger temperatures of all known thermally triggerable SMPs correlate with the respective T_g or T_m. Crosslinking of an amorphous polymer with an unusual broad T_g[8,9] or

co-crosslinking of several amorphous polymers with different T_g[10,11] as well as co-crosslinking of blends of several semi-crystalline polymers with different T_m[12–14] were demonstrated to be suited approaches for realizing multi-shape memory polymers that can stabilize besides a temporary form one or even more intermediate forms. The realization of a triple-shape memory effect by crosslinking of a single semi-crystalline polymer using its T_g and T_m as trigger temperatures was shown also to be possible.[15] Moreover, a triple-shape memory polymer that reacts not only upon exceeding a certain temperature, but also includes the heating rate in its reaction was realized by crosslinking of a syndiotactic polypropylene that can be quenched to a fully amorphous state and offers different crystal modifications with different melting temperatures as potential trigger temperatures.[16]

In contrast to amorphous polymers, semi-crystalline polymers usually have more than one glass transition temperature, which are referred to as relaxation temperatures. For example, polyethylene shows at least three relaxation temperatures; the α-, β-, and γ-relaxation.[17,18] The γ-relaxation for example low-density polyethylene (LDPE) is about $-120°C$ and can be described as a sub-glass relaxation. While above the γ-relaxation temperature the free volume of the amorphous phase allows only the movement of short chain segments,[17,19] it reaches above the β-relaxation temperature ($\approx -20°C$ for LDPE) a degree that allows rotation around the macromolecular backbone and is assumed to be the "classic" glass transition temperature T_g,[20] thus, the movement of larger segments, resulting in the ability of the amorphous phase to be entropy-elastically deformed.[21] However, the nature of the α-relaxation T_α is quite different compared to the two others. Although softening is of course measured in the amorphous phase, the actual origin of T_α is in the crystal. If the temperature exceeds T_α, so-called "twists" (chain twists) can diffuse through lamellar crystals, allowing polymer chains to migrate through crystals and, thus, to rearrange the crystal surface and the interlamellar phase.[22,23] The possibility of chains to migrate through crystals above T_α is considered to be responsible for the increase of the maximum post-stretching ratio with increasing stretching temperature of an already oriented crystallized polymer fiber.[24] Taking this information into account raises the question of whether morphological changes, which take place upon stretching a cross-linked polymer at a temperature above and subsequent constrained cooling below its T_α, can be reversed by re-annealing above T_α. If this were possible T_α could be utilized as novel trigger for shape memory polymers.

The objective of this work is to explore whether a shape memory polymer can be efficiently triggered to switch from one to another shape upon heating above its α-relaxation temperature T_α. Because of its distinctive T_α and ease of crosslinking, we chose LDPE for this purpose.

TABLE 1 Melting temperature T_m, density ρ, and melt flow index (MFI) of low-density polyethylene FA6220.

T_m [°C]	ρ [g/cm^3]	MFI [g/10 min]
111	0.922	2.1

TABLE 2 Melting temperature T_m, density ρ, molar mass M_w, and product purity of dicumyl peroxide.

T_m [°C]	ρ [g/cm^3]	M_w [g/mol]	Purity [%]
39–41	1.02	270.37	98

2 | EXPERIMENTAL

2.1 | Materials

LDPE FA6220 from the manufacturer Borealis serves as raw material for the sample preparation of all samples used in this work. The material data specified by the manufacturer are shown in Table 1.

Dicumyl peroxide (DCP) from the manufacturer Alfa Aesar is used as crosslinking agent for the preparation of cross-linked low-density polyethylene (x-LDPE) samples. The manufacturer data of DCP are listed in Table 2.

2.2 | Sample preparation

The preparation of polyethylene networks was carried out using a micro twin-screw extruder (DSM Research, Inc.) and a heating press (Paul-Otto-Weber Maschinen- & Apparatebau GmbH). For this purpose, LDPE was blended for 5 min with DCP (0.7 wt%) at 120°C. The extruded strands were pelletized, pressed at 160°C to plates of 0.5 mm thickness, and cured for 35 min under exclusion of air. The resulting polyethylene networks were cut into samples of 40 mm length and 10 mm width.

2.3 | Thermal characterization

The degree of crystallinity α_c and the melting temperature T_m of unstretched x-LDPE samples were determined with a differential scanning calorimeter (DSC) (DSC 2910, TA Instruments, Inc.) using a heating rate of 10 K min^{-1}. Sample weights were ranging from 10 to

15 mg. T_m was obtained in peak minimum of the heat flow (exo up). The degree of crystallinity was determined by equation (1), where ΔH_m is the heat of fusion of the sample and $\Delta H_m{}^0 = 289\ J\ g^{-1}$ is the heat of fusion of 100% crystalline polyethylene.

$$\alpha_c = \frac{\Delta H_m}{\Delta H_m^0} \tag{1}$$

A dynamic mechanical analyzer (DMA) (DMA 850, TA Instruments, Inc.) was used to determine the degree of crosslinking x_c and the α-relaxation temperature T_α of cross-linked and unstretched samples. For this purpose, the samples were cut to 20 mm length, mounted in the film-tension clamp of the DMA and analyzed up to a temperature of 160°C with a frequency of 1 Hz, an amplitude of 20 µm, a preload force of 0.2 N and a heating rate of 5 K min^{-1}. x_c was determined according to Flory's theory of viscoelasticity (equation (2)), where M_{rep} is the molecular weight of the repeating unit (28.0528 g/mol), R is the universal gas constant (8.314 J mol^{-1} K^{-1}), $\rho(T)$ is the density, T is the absolute temperature, $E(T)$ is the Young's modulus and ν is the Poisson ratio, which is assumed to be 0.5 above T_m. The equilibrium moduli were determined from the corresponding DMA measurements at 140°C. The sample density was calculated at 140°C to $\rho(T = 140°C) = 0.78\ g\ cm^{-3}$ according to reference[25].

$$x_c = \frac{M_{rep} E(T)}{2 \cdot (1+\nu) \cdot \rho(T) \cdot R \cdot T} \tag{2}$$

2.4 | Microstructural and structural characterization

Small- angle x-ray scattering (SAXS) patterns were recorded with a Bruker Nanostar (Bruker AXS GmbH) consisting of a VANTEC-2000 detector and a micro focus x-ray source (IµS, Incoatec GmbH) with Cu-anode and integrated Montel Optic operated at 50 kV and 0.600 mA. The x-ray wavelength was 0.15406 Å. The sample-to-detector distance was 107 cm. The accumulation time for each frame was 900 s. Silver behenate standard was used for calibrating the scattering angle 2θ. The parameters of the orthorhombic unit cell of polyethylene are $a = 0.741$ nm, $b = 0.494$ nm, $c = 0.255$ nm.

Transmission electron microscopy (TEM) investigations were carried out on a Fisher Scientific Talos F200X G2 transmission electron microscope operated at 200 kV. Ultrathin sections of the cross-linked LDPE samples were prepared with an Leica EM UC7 microtome (Leica Microsymstems GmbH) at a temperature of −130°C and investigated under slight defocus of −5 µm without any staining to avoid artifacts.

2.5 | Determination of shape memory parameters

A strain-controlled custom-made stretching apparatus is used in this work to characterize and determine the shape memory parameters of the LDPE networks. All strains are presented as stretching ratios λ and refer to the initial length of a specimen l_0. The stretching ratios were determined using 1 cm spaced markers on each specimen. The accuracy of the length measurement is ±0.5 mm.

The programming of the samples was carried out as follows: Firstly, the samples were melted at a temperature of 130°C, stretched to a stretching ratio λ_1, and constrained crystallized upon cooling to room temperature T_{RT}. Subsequently, the samples were heated to 80°C, stretched to a stretching ratio λ_2, and cooled constrained to room temperature before the strain fixity ratio R_f ($\lambda_1 \rightarrow \lambda_2$) was determined. λ_1 and λ_2 indicate the intermediate and temporary shapes, respectively. Then, the samples were reheated to 80°C to recover their intermediate shape λ_1' and hold at this temperature for at least 5 min before cooling to room temperature and determining the strain recovery ratio R_r ($\lambda_2 \rightarrow \lambda_1'$). The entire programming process is shown in the following illustration (Figure 1).

The fixity ratio R_f and the recovery ratio R_r were determined using equation (3) and (4).

$$R_f(N) = \frac{\lambda_{fix}(N) - 1}{\lambda_{prog}(N) - 1} \tag{3}$$

$$R_r(Y \rightarrow X)(N) = \frac{\lambda_{Y,fix}(N) - \lambda_{X,rec}(N)}{\lambda_{Y,fix}(N) - \lambda_{X,fix}(N)} \tag{4}$$

X and Y denote two different shapes. λ_{fix} represents the fixed stretching ratio after programming, cooling, and retraction of the stretching force. λ_{rec} is the stretching ratio after triggering. N describes the N^{th} thermomechanical cycle, which the sample has passed.

3 | RESULTS

The objective of this work is to explore whether the α-relaxation temperature T_α can be utilized as trigger to switch a shape memory polymer from one shape to another. We chose LDPE, since it can be easily cross-linked

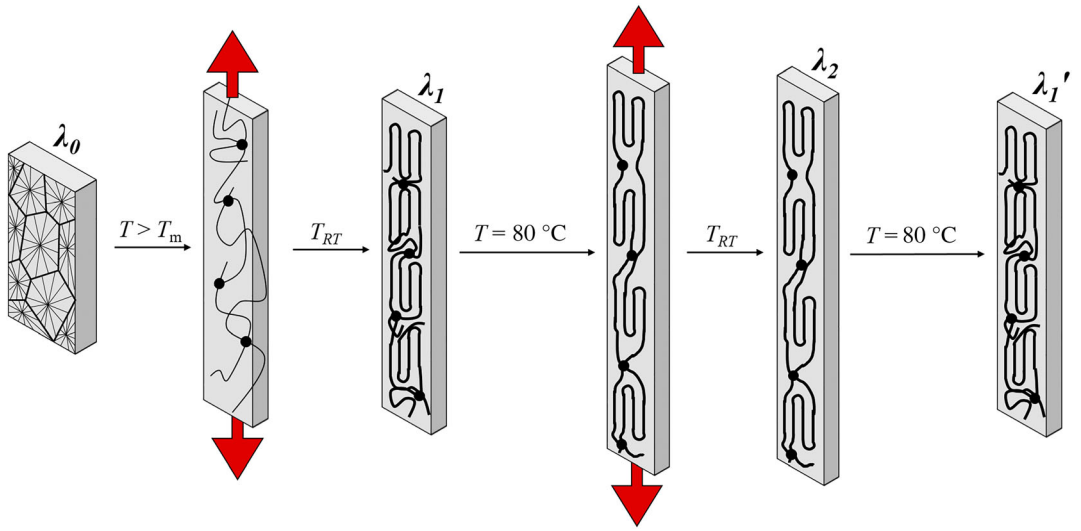

FIGURE 1 Illustration of the programming process of the cross-linked low-density polyethylene samples with stretching ratios λ_0, λ_1, λ_2, and λ_1' indicating the permanent, intermediate, temporary, and recovered intermediate shapes, respectively. [Color figure can be viewed at wileyonlinelibrary.com]

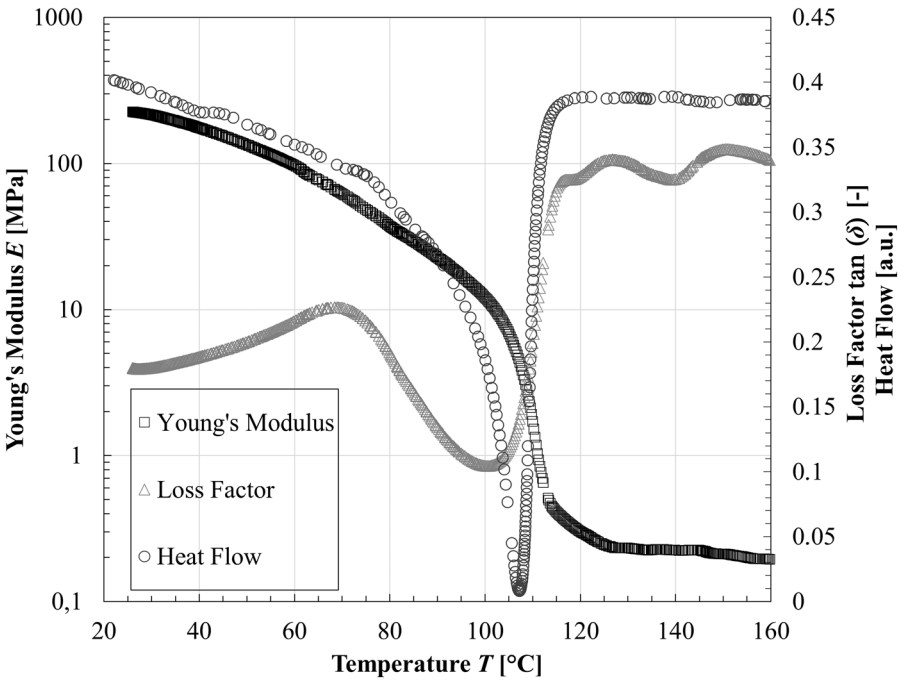

FIGURE 2 DMA and DSC-plots of cross-linked low-density polyethylene cross-linked with 0.7 wt% dicumyl peroxide.

with DCP and offers a distinctive T_α within a reasonable temperature range for many shape memory applications.

First, preliminary tests were carried out to determine the lowest DCP concentration that enables the LDPE network to fully recover ($R_r = 100\%$) its original dimensions, after being stretched above T_m, constrained crystallized upon cooling to room temperature, and re-heated above T_m. We found a DCP concentration of 0.7 wt% suited for this purpose, which corresponds well with previous work.[26] Figure 2 shows the DMA- and DSC-plots of a x-LDPE sample cured with 0.7 wt% DCP.

The plateau of the Young's modulus above T_m proves successful crosslinking of x-LDPE. The degree of crosslinking was calculated from the Young's modulus to $x_c = 0.06\%$ at 140°C. The crystallinity was calculated to $\alpha_c = 37.5\%$. The loss factor tan(δ) clearly shows the temperature range of T_α, which starts at about 40°C, climbs to its maximum at 68°C, and continues up to 90°C. Since all samples ruptured at a stretching ratio just below 10 when stretched at a temperature of 130°C, the following experiments were limited to a maximum stretching ratio λ_{max} of 9.

TABLE 3 Fixity and recovery ratios for the 1st shape memory cycle.

λ_1	λ_2	R_f ($\lambda_0 \rightarrow \lambda_1$) [%]	R_f ($\lambda_1 \rightarrow \lambda_2$) [%]	R_r ($\lambda_1 \rightarrow \lambda_0$) [%]	R_r ($\lambda_2 \rightarrow \lambda_0$) [%]	R_r ($\lambda_2 \rightarrow \lambda_1$) [%]
2	3	100.0	90.5	98.6	99.3	71.8
2	4	100.0	90.4	99.1	99.4	71.4
2	5	100.0	89.9	99.5	99.9	63.3
3	4	100.0	95.8	99.8	99.8	91.1
3	5	100.0	97.5	100.0	100.0	63.2
3	6	100.0	93.1	100.0	100.0	60.2
3	7	100.0	88.6	100.0	100.0	59.0
4	5	100.0	94.1	99.7	100.0	95.6
4	6	100.0	98.0	99.8	100.0	63.2
4	7	100.0	90.0	99.8	99.2	61.4
5	6	100.0	94.7	100.0	100.0	97.0
5	7	100.0	96.7	100.0	100.0	75.4
5	8	100.0	94.1	99.6	99.8	61.1
6	7	100.0	97.2	99.6	99.7	99.8
6	8	100.0	96.5	99.7	99.8	85.0
6	9	100.0	95.9	100.0	100.0	78.4
7	8	100.0	98.7	99.9	99.9	99.4
7	9	100.0	94.7	100.0	100.0	99.0

First experiments regarding the classic shape memory effect using T_m as trigger showed a fixity ratio R_f of 100% after stretching to $\lambda = 9$ at 130°C, subsequent constrained cooling to room temperature, and release of the stretching force. Reheating this sample to 130°C resulted in a recovery ratio R_r of 100%. Expectedly, the same was found for samples constrained crystallized at smaller stretching ratios than 9. This affirms that the network topology of the x-LDPE samples is not altered by a classic shape memory cycle and fulfills the first of the two above-mentioned prerequisites.

In order to explore whether T_α suits as trigger for an SMP, we stretched an x-LDPE sample at a temperature between T_α and T_m from an unoriented spherulitic morphology ($\lambda_0 = 1$) to stretching ratios λ_1 of 2, 4, 6, and 8 and cooled constrained to room temperature. We chose 80°C as stretching temperature because it lies between the average T_α and the average T_m of the melting range of the LDPE crystals (see Figure 2). It turned out that the specimens deformed inhomogeneously under formation of a neck, similar to that known from cold-drawing, and ruptured at a λ between 6 and 8. No specimen even came close to regaining its original dimensions when reheated to 80°C. Interestingly, all samples were capable of fully recovering their initial dimensions upon heating above T_m to a temperature of 130°C. This indicates that the network topology of the x-LDPE samples, although appearing to deform plastically, is not irreversibly altered by the deformation process at 80°C and, thus, only irreversible morphological changes take place upon stretching the spherulitic morphology between T_α and T_m.

Next, we crystallized the x-LDPE samples in an oriented stacked lamellar morphology before stretching them at 80°C. To this end, x-LDPE samples were heated to 130°C, stretched to λ_1 ranging from 2 to 7 and kept constrained while cooling to room temperature. Subsequently, the samples were heated above their average α-relaxation T_α to a temperature of 80°C, stretched to $\lambda_2 = \lambda_1 + n$ with n as a natural number ranging between 1 and 4, and held constrained at this stretching ratio while being cooled to room temperature. During the stretching process from λ_1 to λ_2, it was directly recognizable that the samples elongate uniformly and that a significantly lower stretching force is required compared to that required for drawing of unoriented samples at 80°C.

In order to evaluate the shape memory performance of the prepared x-LDPE samples, they were heated above T_m to a temperature of 130°C to recover their permanent shape $\lambda_0 = 1$ as well as to 80°C to find out whether they are capable of restoring the temporary shape λ_1 in which they were constrained crystallized before. The fixity ratios R_f and recovery ratios R_r between the different shapes were calculated over a total of 5 cycles. The R_f and R_r values determined for the different λ_1/λ_2 combinations are listed in Table 3 only for the 1st shape memory cycle, because no significant variation was found up to the 5th

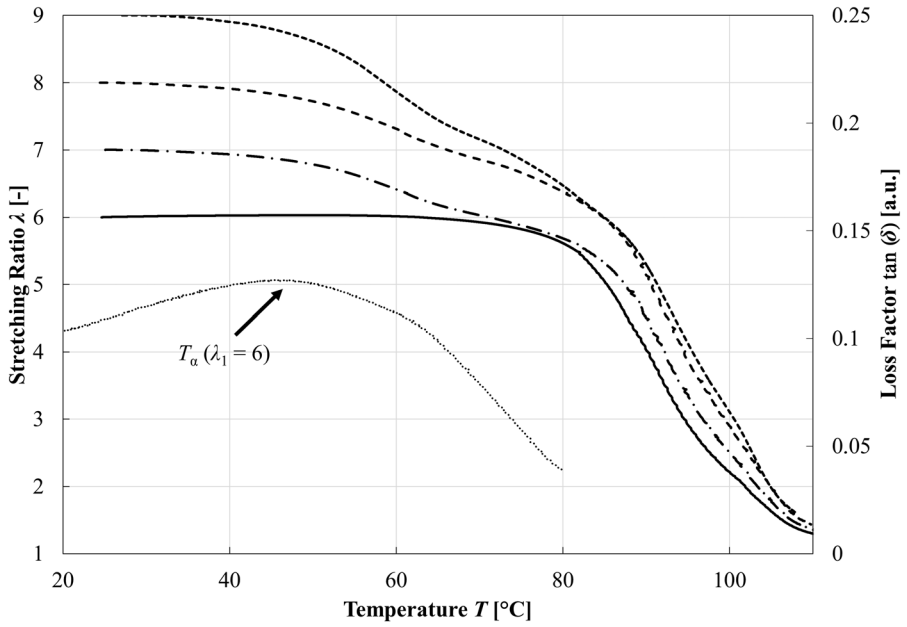

FIGURE 3 Stretching ratio λ versus temperature T plots of an cross-linked low-density polyethylene (x-LDPE) sample constrained crystallized at λ_1 of 6 and of x-LDPE samples that were additionally stretched to λ_2 of 7, 8, and 9 at 80°C after being constrained crystallized at λ_1 of 6. The loss factor tan (δ) versus temperature T plot shows the position of the α-relaxation T_α of an x-LDPE sample constrained crystallized at $\lambda_1 = 6$.

cycle. In case of missing λ_1/λ_2 combinations in Table 3, the samples ruptured during the post-stretching step at 80°C and, thus, were not considered.

As seen in Table 3, all samples were able to almost fully recover their original dimensions upon heating to 130°C independent of the combination of the chosen λ_1 and λ_2 (R_r ($\lambda_{1\ or\ 2} \rightarrow \lambda_0$)≈100%). This indicates that the network topology is still intact after programming of the intermediate shape upon constrained crystallization at λ_1 at 130°C as well as after further programming of the temporary shape upon stretching to λ_2 at 80°C.

Reheating the samples in their temporary shape to 80°C showed that the determined recovery ratios R_r ($\lambda_2 \rightarrow \lambda_1$) strongly depend on the combination of λ_1 and λ_2. Regarding the shape memory parameters determined after stretching from λ_1 to λ_2 and triggering from λ_2 back to λ_1 upon heating to 80°C, it was found that the lower the applied λ_2 at 80°C is, the higher are the determined fixity ratio R_f ($\lambda_1 \rightarrow \lambda_2$) and recovery ratio R_r ($\lambda_2 \rightarrow \lambda_1$).

Besides isothermal triggering of the samples, the trigger process was also investigated continuously upon monitoring the length change in the DMA while heating the samples with a rate of 3 K min^{-1} to a temperature of 130°C. Figure 3 representatively shows the trigger curves of an x-LDPE sample stretched to a λ_1 of 6 at 130°C and constrained crystallized upon cooling to room temperature as well as of samples additionally stretched to λ_2 of 7, 8, and 9 at 80°C after being constrained crystallized at λ_1 of 6.

Figure 3 confirms the fixity and recovery ratios of the x-LDPE samples determined after isothermal tempering at 80°C and clearly shows that only the x-LDPE sample stretched from $\lambda_1 = 6$ to $\lambda_2 = 7$ at 80°C is capable of nearly 100% recovering its prior strain ratio λ_1 upon heating again to 80°C. It can be also seen that all samples, which were additionally stretched to λ_2 at 80°C start to trigger back to $\lambda_1 = 6$ in the range of T_α (see tan(δ) in Figure 3) while the sample solely constrained crystallized at $\lambda_1 = 6$ shows no reaction within this temperature range. This is a first indication that triggering of post-stretched samples from λ_2 back to λ_1 could indeed be related to T_α.

SAXS experiments were carried out with x-LDPE samples in their intermediate, temporary, and recovered intermediate shapes to gain information about the mechanism of the novel shape memory switch. Figure 4 shows the recorded SAXS patterns of x-LDPE samples at $\lambda_1 = 6$, $\lambda_2 = 7$, 8, and 9, and the respective λ_1' after triggering upon heating to 80°C as well as after a second shape memory cycle from λ_1' to λ_2 and back to λ_1''.

As seen in Figure 4, the SAXS patterns of the samples constrained crystallized at a λ_1 of 6 change only slightly upon stretching to a λ_2 of 7 at 80°C, while the SAXS patterns after stretching to λ_2 of 8 and 9 at 80°C change distinctly. Upon reheating to 80°C, only the x-LDPE stretched to a λ_2 of 7 recovers its prior SAXS pattern. This indicates that the morphology of the sample with a λ_1/λ_2 combination of 6/7 is restored, which is in good accordance with the determined recovery ratio listed in Table 3. For the remaining two combinations (6/8 and 6/9), reheating to 80°C leads again to a characteristic stacked lamellar morphology, but in which smaller long periods are missing. Interestingly, the SAXS patterns taken after a second shape memory cycle between temporary and intermediate shape ($\lambda_1' \rightarrow \lambda_2 \rightarrow \lambda_1''$) indicate that the morphology is restored. A review of the recovery

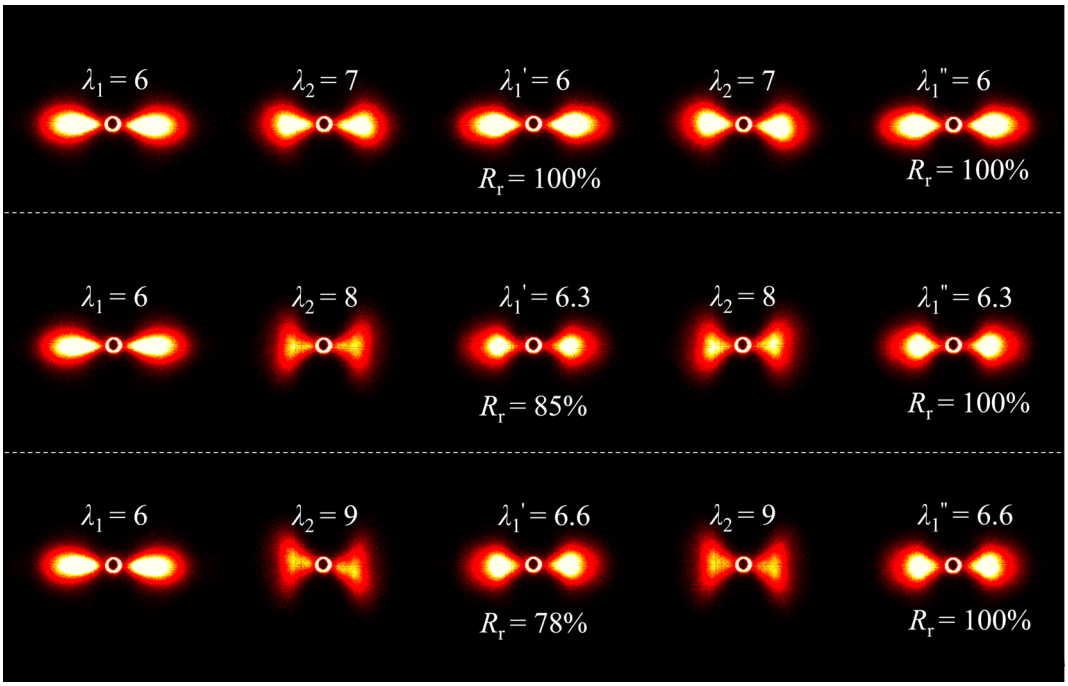

FIGURE 4 Small- angle x-ray scattering patterns of the intermediate, temporary, and recovered intermediate shapes of cross-linked low-density polyethylene samples for different λ_1/λ_2 combinations. [Color figure can be viewed at wileyonlinelibrary.com]

ratios R_r ($\lambda_2 \rightarrow \lambda_1''$) showed that after this first shape memory cycle all irreversible processes take place, so that after the second shape memory cycle the intermediate shape can be restored to 100% for all investigated λ_1/λ_2 combinations. This confirms that in case of x-LDPE the α-relaxation is at least after performing of a first "conditioning" cycle a suited and efficient trigger for switching between a temporary and an intermediate shape. It is particularly interesting that this effect is obviously based on a reversible morphological change.

Based on these findings, we hypothesize that the migration of chains through crystals above the α-relaxation temperature is responsible for the observed shape memory effect. In case of moderate stretching (e.g. $\lambda_1 = 6 \rightarrow \lambda_2 = 7$) at 80°C, we assume that loose tie molecules between lamellae crystals become strained and subsequently subjected to tensile stress (see Figure 5 (top)). This stress forces chains to slip through the crystals and leads to tightening of existing loose loops at the opposite crystal face. Since the migration of chains through crystals is no longer possible below T_α, the release of the stretching force causes only a partial relaxation of the tie chains between crystals and fixes the x-LDPE sample in the temporary shape. Reheating the sample above T_α enables again the migration of chains and allows tight folds to re-expand upon pulling chains through the crystals, which in turn leads to a shortening of the tie molecules on the opposite side and consequently to a reduction of the distance between the lamellar crystals.

In case of more intense stretching at 80°C (e.g. $\lambda_1 = 6 \rightarrow \lambda_2 = 9$), the SAXS patterns of the intermediate and temporary shapes suggest a change from a classical to a stacked lamellar morphology that consists of displaced lamellae crystals (see Figure 5 (bottom)).[27] We assume that differently long strained tie molecules introduce inhomogeneous stress into the crystals, which is responsible for shearing and displacing of the lamellae. When the stretching force is released after cooling below T_α, the sample stabilizes in an elongated temporary shape and mostly recovers its prior intermediate shape only when being reheated above T_α. As indicated by SAXS the sample also recovers its prior morphology upon reheating above T_α. This indicates that the morphology changes between the intermediate and the temporary shape somehow correlate with the α-relaxation. We suggest that the recovery process of the intermediate shape is caused by the relaxation of strained tie molecules between crystals and a shear back of the displaced lamellae driven by the minimization of crystal surface.

TEM was carried out to confirm the morphology changes suggested by SAXS. Figure 6 representatively shows the transmission electron micrographs of an x-LDPE sample that was (a) constrained crystallized at $\lambda_1 = 6$, (b) than stretched to $\lambda_2 = 8$ at 80°C and subsequently cooled to room temperature, and (c) finally

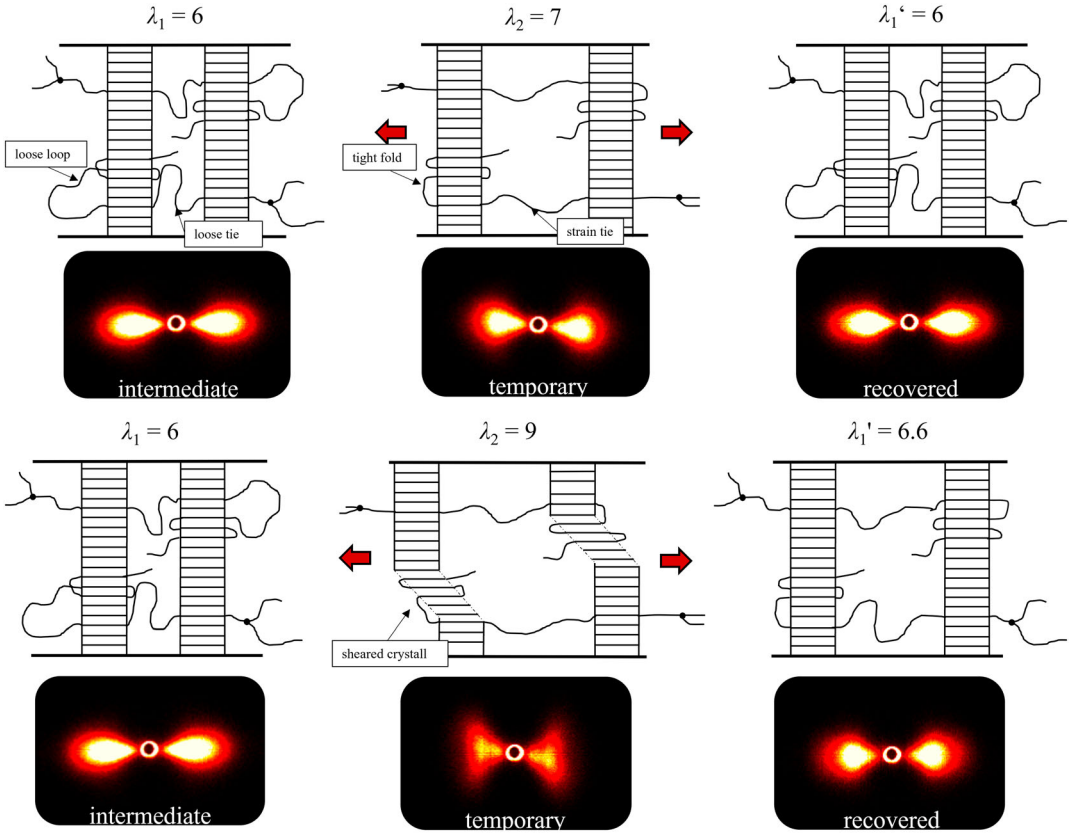

FIGURE 5 Assumed mechanism of the α-relaxation based shape memory effect for moderate (top) and intense stretching (bottom) of cross-linked low-density polyethylene at 80°C. [Color figure can be viewed at wileyonlinelibrary.com]

reheating to 80°C and cooled to room temperature. While the morphologies of x-LDPE in the intermediate (λ_1) as well as in the recovered intermediate shape (λ_1') consist of straight lamellae partially visible throughout the entire image, shorter lamellar crystals partially displaced upon shear could be observed in the x-LDPE after stretching to the temporary shape (λ_2).

Finally, SAXS measurements were carried out with x-LDPE samples after exaggerated stretching at 80°C to gain information about the reason why such samples show only poor recovery after reheating above T_α. As seen in Figure 7, the stacked lamellar morphology of the intermediate shape changes significantly upon exaggerated stretching and does not even close return to the prior stacked lamellar morphology upon reheating above T_α. The SAXS patterns recorded for exaggeratedly stretched and reheated x-LDPE samples suggest that the stacked lamellar morphology transforms into a fiber-typical fibrillar morphology[27–29] comprised of small crystals separated from each other. This points out, that proper recovery ratios R_r ($\lambda_2 \rightarrow \lambda_1$) can only be achieved as long as the crystals of the stacked lamellar morphology are only sheared and not separated into fibrils upon stretching at 80°C.

4 | CONCLUSION

Using the example of cross-linked x-LDPE, we were able to demonstrate that the α-relaxation T_α can be successfully utilized as trigger to switch a cross-linked semicrystalline thermoplastic from one shape to another. However, it is mandatory to crystallize x-LDPE constrained to fix it in an intermediate shape. The programming of the temporary shape occurs upon stretching at a temperature between the α-relaxation T_α and the melting temperature T_m of x-LDPE. Reheating to this temperature initiates the recovery of the intermediate shape. While in case of moderate stretching at 80°C the intermediate shape is fully recovered after the first shape memory cycle, samples that were intensively stretched need a first "conditioning" shape memory cycle before they are able to fully recover the intermediate shape. However, heating above T_m causes for all observed λ_1/λ_2 combinations full recovery of the original dimensions of the x-LDPE sample. We found that switching between the intermediate and the temporary shape is related to a reversible morphology change that is based on the migration of chains through the lamellar crystals above T_α.

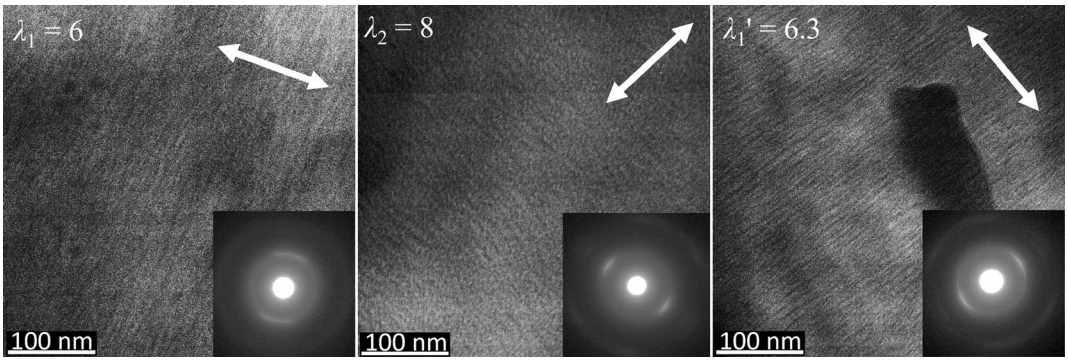

FIGURE 6 Transmission electron micrographs of cross-linked low-density polyethylene after constrained crystallization in the intermediate shape (λ_1), after stretching to the temporary shape (λ_2) at 80°C, and subsequent cooling to room temperature, as well as after recovering the intermediate shape (λ_1') upon reheating to 80°C and cooling to room temperature.

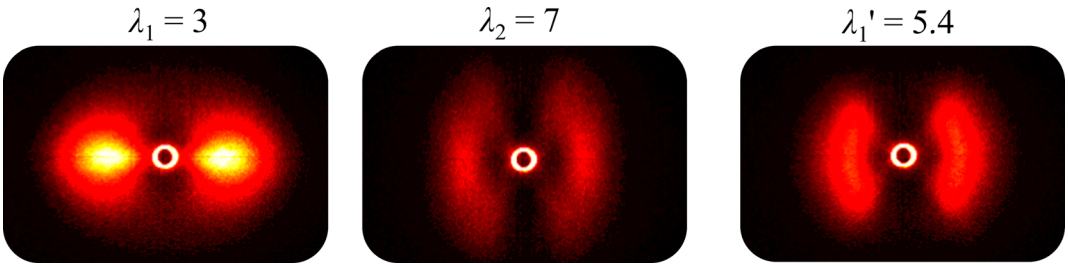

FIGURE 7 Small- angle x-ray scattering patterns of an cross-linked low-density polyethylene sample constrained crystallized at $\lambda_1 = 3$ (left), after exaggerated stretching to $\lambda_2 = 7$ at 80°C (middle), and after reheating to 80°C (right). [Color figure can be viewed at wileyonlinelibrary.com]

Although, all findings in this paper indicate that the α-relaxation is indeed responsible for the presence of the intermediate shape there is a slight possibility that also melting of small crystal fractions might play a role for the observed effect, since the used LDPE has an extremely wide melting range, which already begins below the T_α peak temperature. For this reason, future investigations will focus on other thermoplastics whose melting and α-relaxation ranges do not overlap in order to test whether a triple-shape memory effect can actually be realized with T_α for every semi-crystalline thermoplastic and whether the effect observed in this work can actually be attributed to the α-relaxation alone.

AUTHOR CONTRIBUTIONS

Michail Maricanov: Conceptualization (supporting); data curation (lead); methodology (lead); writing – review and editing (equal). **Roman Becker:** Data curation (supporting); methodology (supporting). **Robert David Ludwig Jerusalem:** Data curation (supporting); methodology (supporting). **Joerg Christian Tiller:** Writing – review and editing (supporting). **Frank Katzenberg:** Conceptualization (lead); writing – review and editing (lead).

ACKNOWLEDGMENTS

The authors acknowledge the funding provided by the Deutsche Forschungsgemeinschaft DFG under grand KA 1813/5-1. The TEM was in part financed by the DFG under grant INST 212/423-1 FUGG. Open Access funding enabled and organized by Projekt DEAL.

DATA AVAILABILITY STATEMENT

The data that support the findings of this study are available from the corresponding author upon reasonable request.

ORCID

Joerg Christian Tiller https://orcid.org/0000-0002-1531-0795

Frank Katzenberg https://orcid.org/0000-0001-6585-5534

REFERENCES

[1] A. Lendlein, S. Kelch, *Angew. Chem. Int. Ed. Engl.* **2002**, *41*, 2034.

[2] Y. Liu, K. Gall, M. L. Dunn, A. R. Greenberg, J. Diani, *Int. J. Plast.* **2006**, *22*, 279.

[3] D. Ratna, J. Karger-Kocsis, *J. Mater. Sci.* **2008**, *43*, 254.

[4] J. Hu, Y. Zhu, H. Huang, J. Lu, *Prog. Polym. Sci.* **2012**, *37*, 1720.
[5] D. Quitmann, M. Dibolik, F. Katzenberg, J. C. Tiller, *Macromol. Mater. Eng.* **2015**, *300*, 25.
[6] F. Katzenberg, J. C. Tiller, *J. Polym. Sci. B Polym. Phys.* **2016**, *54*, 1381.
[7] A. J. Rosario, B. R. Ma, *ACS Appl. Polym. Mater.* **2024**. Epub ahead of print.
[8] T. Xie, *Nature* **2010**, *464*, 267.
[9] S. Billa, P. Vislavath, J. Bahadur, S. K. Rath, D. Ratna, N. R. Manoj, B. C. Chakraborty, *ACS Appl. Polym. Mater.* **2023**, *5*, 3079.
[10] C. Samuel, S. Barrau, J.-M. Lefebvre, J.-M. Raquez, P. Dubois, *Macromolecules* **2014**, *47*, 6791.
[11] Y. Wang, J. Li, X. Li, Y. Pan, Z. Zheng, X. Ding, Y. Peng, *RSC Adv.* **2014**, *4*, 20364.
[12] R. Hoeher, T. Raidt, C. Krumm, M. Meuris, F. Katzenberg, J. C. Tiller, *Macromol. Chem. Phys.* **2013**, *214*, 2725.
[13] D. Ratna, J. Karger-Kocsis, *Polymer* **2011**, *52*, 1063.
[14] S. Jagtap, V. Dalvi, K. Sankar, D. Ratna, *Polym. Int.* **2019**, *68*, 812.
[15] S. Ji, J. Wang, A. Olah, E. Baer, *J. Appl. Polym. Sci.* **2017**, *134*, 44405.
[16] R. Hoeher, T. Raidt, F. Katzenberg, J. C. Tiller, *ACS Appl. Mater. Interfaces* **2016**, *8*, 13684.
[17] R. H. Boyd, *Polymer* **1985**, *26*, 1123.
[18] I. M. Ward, J. Sweeney, *Mechanical properties of solid polymers*, John Wiley & Sons, Chichester, United Kingdom **2012**.
[19] W. Pechhold, S. Blasenbrey, S. Woerner, *Kolloid Z Z Polym.* **1963**, *189*, 14.
[20] U. W. Gedde, M. S. Hedenqvist, *Fundamental polymer science*, Springer, Cham, Switzerland **2019**.
[21] R. Boyd, A. Hasan, *Polymer* **1984**, *25*, 347.
[22] R. Popli, M. Glotin, L. Mandelkern, R. Benson, *J. Polym. Sci., Polym. Phys. Ed.* **1984**, *22*, 407.
[23] K. Schmidt-Rohr, H. Spiess, *Macromolecules* **1991**, *24*, 5288.
[24] W. G. Hu, K. Schmidt-Rohr, *Acta Polym.* **1999**, *50*, 271.
[25] R. A. Orwoll, P. J. Flory, *J. Am. Chem. Soc.* **1967**, *89*, 6814.
[26] R. Hoeher, T. Raidt, M. Rose, F. Katzenberg, J. C. Tiller, *J. Polym. Sci., Part B: Polym. Phys.* **2013**, *51*, 1033.
[27] V. Marikhin, L. Myasnikova, *Orientational Phenomena in Polymers. Prog. Colloid Polym. Sci.* **1993**, *92*, 39.
[28] L. Alexander, *X-ray diffraction methods in polymer science*, Wiley-Interscience, New York, USA **1971**.
[29] M. Kakudo, N. Kasai, *X-ray Diffraction by Polymers*, Kodansha/Elsevier, Tokyo, Japan/Amsterdam, Netherlands **1972**.

How to cite this article: M. Maricanov, R. Becker, R. D. L. Jerusalem, J. C. Tiller, F. Katzenberg, *J. Appl. Polym. Sci.* **2024**, *141*(46), e56241. https://doi.org/10.1002/app.56241